arXiv:1404.2996v4 [hep-ph] 2 Oct 2014

Inert Dark Matter in Type-II Seesaw

Chuan-Hung Chen[a*] **and Takaaki Nomura**[a†]

[a] *Department of Physics, National Cheng-Kung University, Tainan 701, Taiwan*

(Dated: October 3, 2014)

Abstract

Weakly interacting massive particle (WIMP) as a dark matter (DM) candidate is further inspired by recent AMS-02 data, which confirm the excess of positron fraction observed earlier by PAMELA and Fermi-LAT experiments. Additionally, the excess of positron+electron flux is still significant in the measurement of Fermi-LAT. For solving the problems of massive neutrinos and observed excess of cosmic-ray, we study the model with an inert Higgs doublet (IHD) in the framework of type-II seesaw model by imposing a Z_2 symmetry on the IHD, where the lightest particle of IHD is the DM candidate and the neutrino masses originate from the Yukawa couplings of Higgs triplet and leptons. We calculate the cosmic-ray production in our model by using three kinds of neutrino mass spectra, which are classified by normal ordering, inverted ordering and quasi-degeneracy. We find that when the constraints of DM relic density and comic-ray antiproton spectrum are taken into account, the observed excess of positron/electron flux could be explained well in normal ordered neutrino mass spectrum. Moreover, excess of comic-ray neutrinos is implied in our model. We find that our results on $\langle \sigma v \rangle$ are satisfied with and close to the upper limit of IceCube analysis. More data from comic-ray neutrinos could test our model.

* Email: physchen@mail.ncku.edu.tw

† Email: numura@mail.ncku.edu.tw

I. INTRODUCTION

Two strong direct evidences indicate the existence of new physics: one is the observations of neutrino oscillations, which lead to massive neutrinos [1], and another one is the astronomical evidence of dark matter (DM), where a weakly interacting massive particle (WIMP) is the candidate in particle physics. The Planck best-fit for the DM density, which combines the data of WMAP polarization at low multipoles, high-ℓ experiments and baryon acoustic oscillations (BAO), etc., now is given by [2]

$$\Omega h^2 = 0.1187 \pm 0.0017\,. \tag{1}$$

Until now, we have not concluded what the DM is and what the masses of neutrinos originate. It is interesting if we can accommodate both DM issue and neutrino masses in the same framework.

Although the probe of DM could be through the direct detection experiments, however according to the recent measurements by LUX Collaboration [3] and XENON100 [4], we are still short of clear signals and the cross section for elastic scattering of nuclei and DM has been strictly limited. In contrast, the potential DM signals have been observed by the indirect detections. For instance, the recent results measured by AMS-02 [5] have confirmed the excess of positron fraction which was observed earlier by PAMELA [6] and Fermi-LAT [7] experiments. Additionally, the excess of positron+electron flux above the calculated backgrounds is also observed by PAMELA [8], Fermi-LAT [9], ATIC [10] and HESS [11, 12]. Inspired by the observed anomalies, various interesting possible mechanisms to generate the high energy positrons and electrons are proposed, such as pulsars [13, 14], dark matter annihilations [15–17] and dark matter decays [18–20].

The origin of neutrino masses is one of most mysterious problems in high energy physics. Before nonzero neutrino masses were found, numerous mechanisms had been proposed to understand the source of neutrino masses, such as type-I seesaw [21] and type-II seesaw [22, 23] mechanisms, where the former introduced the heavy right-handed neutrinos and the latter extended the standard model (SM) by including a $SU(2)$ Higgs triplet. Since the triplet scalars only couple to leptons, based on this character, it may have interesting impacts on the cosmic-ray positrons, electrons and neutrinos. We therefore study a simple extension of conventional type-II seesaw model by including the possible DM effects.

For studying the excess of cosmic rays by DM annihilation and the masses of neutrinos, we add an extra Higgs doublet (Φ) and a Higgs triplet (Δ) to the SM. Besides the gauge symmetry $SU(2)_L \times U(1)_Y$, in order to get a stable DM, we impose a discrete Z_2 symmetry in our model, where the Φ is Z_2-odd and the Δ and SM particles are Z_2-even. The Z_2 odd doublet is similar to the one in inert Higgs doublet (IHD) model [24, 25], where the IHD model has been studied widely in the literature, such as DM direct detection [25–27], cosmic-ray gamma spectrum [28], cosmic-ray positrons and antiproton fluxes [29], collider signatures [30, 31], etc. The lightest neutral odd particle could be either CP-odd or CP-even, in this work we will adopt the CP-even boson as the DM candidate. For explaining the observed excess of cosmic rays, we set the odd particle masses at TeV scale.

There are two motivations to introduce the Higgs triplet. First, like the type-II seesaw mechanism [22, 23], the small neutrino masses could be explained by the small VEV of triplet without introducing heavy right-handed neutrinos. Second, the excess of cosmic-ray appears in positrons and electrons, however, by the measurements of AMS [32], PAMELA [33] and HESS [34], no excess is found in cosmic-ray antiproton spectrum. Since triplet Higgs bosons interact with leptons but do not couple to quarks, it is interesting to explore if the observed excess of positron fraction and positron+electron flux could be explained by the leptonic decays of Higgs triplet in DM annihilation processes. The model with one odd singlet and one $SU(2)_L$ triplet has been studied and one can refer to Ref. [35]. Furthermore, the search of doubly charged Higgs now is an important topic at colliders. If doubly charged Higgs is 100% leptonic decays, the experimental lower bound on its mass has been limited in the range between 375 and 409 GeV [40, 41]. The detailed analysis and the implications at collider physics could consult the Refs. [36–39].

The decays of triplet particles to leptons depend on the Yukawa couplings. As known, the Yukawa couplings could be constrained by the measured neutrino mass-squared differences and the mixing angles of Pontecorvo-Maki-Nakagawa-Sakata (PMNS) matrix [42, 43], where the current data are given by [1]

$$\begin{aligned}
\Delta m^2_{21} &= (7.50 \pm 0.20) \times 10^{-5} eV^2 \,, \\
|\Delta m^2_{31}| &= (2.32^{+0.12}_{-0.08}) \times 10^{-3} eV^2 \,, \\
\sin^2(2\theta_{12}) &= 0.857 \pm 0.024 \,, \sin^2(2\theta_{23}) > 0.95 \,, \\
\sin^2(2\theta_{13}) &= 0.095 \pm 0.01. \qquad (2)
\end{aligned}$$

Since the data can not tell the mass pattern from various neutrino mass spectra, in our study, we classify the mass spectra to be normal ordering (NO), inverted ordering (IO) and quasi-degeneracy (QD) [1] and investigate their influence on the production of cosmic rays. Because we do not have any information on the Dirac (δ) and Majorana ($\alpha_{31,21}$) phases in PMNS matrix, we adopt four benchmark points that are used by CMS Collaboration for the search of doubly charged Higgs [40]. The first three benchmark points stand for the NO, IO and QD with $\delta = \alpha_{31} = \alpha_{21} = 0$ while the fourth one denotes the QD with $\delta = \alpha_{31} = 0$ and $\alpha_{21} = 1.7$. We note that the necessary boost factor (BF) for fitting the measured cosmic-ray electron/positron flux by DM annihilation is regarded as astrophysical effects [44]. We take the BF as a parameter and use the data of antiproton spectrum to bound it.

Furthermore, since the singly charged and neutral triplet particles couple to neutrinos, an excess of cosmic-ray neutrinos is expected in the model. We find that a Breit-Wigner enhancement could occur at the production of neutrinos; therefore, without BF, a large neutrino flux from DM annihilation could be accomplished. Accordingly, with the same values of free parameters that fit the excess of cosmic-ray positron/electron flux, our results on neutrino excess from galactic halo could be close to the upper bound measured by IceCube [45, 46].

The paper is organized as follows. We introduce the gauge interactions of IHD and triplet, Yukawa couplings of triplet, and scalar potential in Sec II. The set of free parameters and the branching fractions of triplet particle decays are introduced in Sec III. In Sec IV, we discuss the constraints from relic density of DM and cosmic-ray antiproton spectrum. With the values of constrained parameters, we study the fluxes of cosmic-ray positrons, electrons and neutrinos. We give a summary in Sec V.

II. INERT HIGGS DOUBLET IN TYPE-II SEESAW MODEL

In this section, we introduce the new interactions in the model. In order to have a stable DM, we consider the symmetry $SU(2)_L \times U(1)_Y \times Z_2$. For generating the masses of neutrinos and having a DM candidate, we extend the SM to include a scalar triplet Δ with hypercharge $Y = 2$ and a scalar doublet Φ with hypercharge $Y = 1$. The SM particles and the triplet Δ are Z_2-parity even while the new doublet Φ is Z_2-parity odd. Since the DM does not decay in the model, therefore, Φ cannot develop a VEV when electroweak symmetry is broken.

The couplings in the SM are well known, therefore we do not further discuss them. With the new Z_2-parity, the involved new gauge interactions, new Yukawa couplings and scalar potential are written as

$$\mathcal{L}_{NP} = (D_\mu \Phi)^\dagger D^\mu \Phi + (D_\mu \Delta)^\dagger D^\mu \Delta - \left[\frac{1}{2} L^T C(\mathbf{y} + \mathbf{y^T}) i\sigma_2 \Delta P_L L + h.c.\right] - V(H, \Phi, \Delta)\,, \quad (3)$$

where we have suppressed the flavor indices in Yukawa sector, $\mathbf{y}$ denotes the 3×3 Yukawa matrix, $P_L = (1-\gamma_5)/2$, $L^T = (\nu_\ell, \ell)$ is the lepton doublet, σ_2 is the second Pauli matrix and $C = i\gamma_0\gamma_2$. Due to Φ being Z_2 odd, it cannot couple to SM fermions. The representations for SM Higgs doublet H, Φ and triplet are chosen as

$$\begin{aligned} H &= \begin{pmatrix} G^+ \\ (v_0 + h + iG^0)/\sqrt{2} \end{pmatrix}, \quad \Phi = \begin{pmatrix} H^+ \\ (S + iA)/\sqrt{2} \end{pmatrix}, \\ \Delta &= \begin{pmatrix} \delta^{++} \\ \delta^+ \\ (v_\Delta + \delta^0 + i\eta^0)/\sqrt{2} \end{pmatrix} \text{ or } \begin{pmatrix} \delta^+/\sqrt{2} & \delta^{++} \\ (v_\Delta + \delta^0 + i\eta^0)/\sqrt{2} & -\delta^+/\sqrt{2} \end{pmatrix}, \end{aligned} \quad (4)$$

where $v_{0(\Delta)}$ are the VEV of neutral component of $H(\Delta)$ and their values are related to the parameters of scalar potential. There are two ways to present Δ: for gauge interactions we use 3×1 column vector but for Yukawa couplings and scalar potential, we use 2×2 matrix. Since the mixing of H and Δ is related to the small v_Δ, which is constrained by ρ parameter and the masses of neutrinos, the Goldstone bosons and Higgs boson are mainly from the SM Higgs doublet. Below we discuss each sector individually.

A. Gauge Interactions

The covariant derivatives for scalar doublet and triplet could be expressed by

$$D_\mu = \partial_\mu + i\frac{g}{\sqrt{2}}\left(\mathbf{T}^+ W_\mu^+ + \mathbf{T}^- W_\mu^-\right) + i\frac{g}{c_W}\left(\mathbf{T^3} - s_W^2 \mathbf{Q}\right) Z_\mu + ie\mathbf{Q}A_\mu\,. \quad (5)$$

The $W_\mu^\pm$, Z_μ and A_μ stand for the gauge bosons in the SM, g is the gauge coupling of $SU(2)_L$ and $s_W(c_W) = \sin\theta_W(\cos\theta_W)$ with θ_W being the Weinberg angle. For scalar doublet, $\mathbf{T}^\pm = (\sigma^1 \pm i\sigma^2)/2$ and $\mathbf{T^3} = \sigma^3$ are associated with Pauli matrices and diag$\mathbf{Q} = (1, 0)$ is the charge operator. For scalar triplet, the charge operator is diag$\mathbf{Q} = (2, 1, 0)$, $\mathbf{T}^\pm = T_1 \pm iT_2$

and the generators of $SU(2)$ are set to be

$$T_1 = \frac{1}{\sqrt{2}} \begin{pmatrix} 0 & 1 & 0 \\ 1 & 0 & 1 \\ 0 & 1 & 0 \end{pmatrix} \ , \ T_2 = \frac{1}{\sqrt{2}} \begin{pmatrix} 0 & -i & 0 \\ i & 0 & -i \\ 0 & i & 0 \end{pmatrix} \ , \ T_3 = \begin{pmatrix} 1 & 0 & 0 \\ 0 & 0 & 0 \\ 0 & 0 & -1 \end{pmatrix} \ . \tag{6}$$

The kinetic terms of SM Higgs and Δ will contribute to the masses of $W^{\pm}$ and Z bosons. After spontaneous symmetry breaking (SSB), the masses of $W^{\pm}$ and Z bosons are given by

$$\begin{aligned} m_W^2 &= \frac{g^2 v_0^2}{4} \left(1 + \frac{2v_\Delta^2}{v_0^2} \right) , \\ m_Z^2 &= \frac{g^2 v_0^2}{4 \cos^2 \theta_W} \left(1 + \frac{4v_\Delta^2}{v_0^2} \right) . \end{aligned} \tag{7}$$

As a result, the ρ-parameter at tree level could be obtained as

$$\rho = \frac{m_W^2}{m_Z^2 c_W^2} = \frac{1 + 2v_\Delta^2/v_0^2}{1 + 4v_\Delta^2/v_0^2} \, . \tag{8}$$

Taking the current precision measurement for ρ-parameter to be $\rho = 1.0004^{+0.0003}_{-0.0004}$ [1], we get $v_\Delta < 3.4$ GeV when 2σ errors is taken into account.

We find that the gauge interactions of triplet particles such as $\delta^0 W^+ W^-$ and $\delta^0 ZZ$, which will be directly related to the relic density and excess of cosmic rays, are all proportional to v_Δ. For small v_Δ, the effects are negligible. It is known that triplet particles have two main decay channels: one is decaying to paired gauge bosons and the other is leptonic decays. In order to obtain the excess of cosmic-ray positrons/electrons and avoid getting a large cosmic-ray antiproton spectrum, the paired gauge boson channel should be suppressed. For achieving the purpose, we take $v_\Delta < 10^{-4}$ GeV [37]. Although the vertex of $ZY\bar{Y}$ with $Y = \delta^{(++,+)}$ is important to produce the pair of triplet particles, however the (co)annihilation through the couplings of H^+H^-A, H^+H^-Z and SAZ is suppressed by the low momenta of odd particles. Therefore, their effects are not significant.

In order to satisfy the measured relic density Ωh^2 and produce interesting excess of cosmic rays, the important gauge interactions are only associated with odd particles. The relevant

interactions are written as

$$\begin{aligned}\mathcal{L}_G \;=\; & -\frac{g}{2}\left(S(p_S-p_{H^-})^\mu + iA(p_A-p_{H^-})^\mu\right)W_\mu^+ H^- - i\frac{g}{2\cos\theta_W}(p_S-p_A)^\mu Z_\mu AS \\ & + \left[\frac{g}{2}(S-iA)H^+W_\mu^-\left(eA^\mu + \frac{g\sin^2\theta_W}{\cos^2\theta_W}Z^\mu\right) + h.c.\right] \\ & + H^+H^-\left(eA^\mu + \frac{g\cos 2\theta_W}{\cos\theta_W}Z^\mu\right)^2 + \frac{g^2}{4}(S^2+A^2)W_\mu^+W^{-\mu} \\ & + \frac{g^2}{8\cos^2\theta_W}(S^2+A^2)Z_\mu Z^\mu\,. \end{aligned} \tag{9}$$

According to Eq. (9), we see that the DM (co)annihilation could produce W^+W^- and ZZ pairs by s- and t-channel. Although the W^+W^- and ZZ pairs are open in the model and will contribute to the antiproton flux, however, we will see that the produced antiprotons in the energy range of observations are still consistent with data measured by AMS [32], PAMELA [33] and HESS [34].

B. Yukawa Couplings

Next, we discuss the origin of neutrino masses and new lepton couplings in the model. Using the 2×2 representation for Δ, the Yukawa interactions in Eq. (3) could be decomposed as

$$\begin{aligned} -\mathcal{L}_Y \;=\; & \frac{1}{2}\nu^T C\mathbf{h}P_L\nu\frac{v_\Delta+\delta^0+i\eta^0}{\sqrt{2}} - \nu^T C\mathbf{h}P_L\ell\frac{\delta^+}{\sqrt{2}} \\ & -\frac{1}{2}\ell^T C\mathbf{h}P_L\ell\delta^{++} + h.c. \end{aligned} \tag{10}$$

where $\bar{\mathbf{h}} = \mathbf{y} + \mathbf{y^T}$ and it is a symmetric 3×3 matrix. Clearly, the neutrino mass matrix is given by $\mathbf{m}_\nu = v_\Delta\mathbf{h}/\sqrt{2}$. For explaining the tiny neutrino masses, we can adjust the v_Δ and $\mathbf{h}$. In this paper, for suppressing the triple couplings of triplet particle and gauge bosons so that the leptonic triplet decays are dominant, we adopt $v_\Delta < 10^{-4}$ GeV [37]. By using PMNS matrix [42, 43], the Yukawa couplings could be determined by the neutrino masses and the elements of PMNS matrix. The relation is given by

$$\mathbf{h} = \frac{\sqrt{2}}{v_\Delta}U^*_{\rm PMNS}\mathbf{m}_\nu^{\rm dia}U^\dagger_{\rm PMNS}\,, \tag{11}$$

where $\mathbf{m}_\nu^{\rm dia} = {\rm diag}(m_1, m_2, m_3)$, m_is are the physical masses of neutrinos and PMNS matrix is parametrized by [1]

$$U_{\rm PMNS} = \begin{pmatrix} c_{12}c_{13} & s_{12}c_{13} & s_{13}e^{-i\delta} \\ -s_{12}c_{23} - c_{12}s_{23}s_{13}e^{i\delta} & c_{12}c_{23} - s_{12}s_{23}s_{13}e^{i\delta} & s_{23}c_{13} \\ s_{12}s_{23} - c_{12}c_{23}s_{13}e^{i\delta} & -c_{12}s_{23} - s_{12}c_{23}s_{13}e^{i\delta} & c_{23}c_{13} \end{pmatrix} \times {\rm diag}(1, e^{i\alpha_{21}/2}, e^{i\alpha_{31}/2}) \tag{12}$$

with $s_{ij} \equiv \sin\theta_{ij}$, $c_{ij} \equiv \cos\theta_{ij}$ and $\theta_{ij} = [0, \pi/2]$. $\delta = [0, \pi]$ is the Dirac CP violating phase and $\alpha_{21,31}$ are Majorana CP violating phases. According to Eq. (10), the couplings of triplet particles to SM leptons are all related to $\mathbf{h}$, therefore the Yukawa couplings of $\delta^{\pm\pm}$, $\delta^\pm$ and $\delta^0(\eta^0)$ are limited by the neutrino experiments. If we set $v_\Delta h_{\ell'\ell}/\sqrt{2} = m_{\ell'\ell}$, the Eq. (11) could be decomposed as

$$\begin{aligned}
m_{ee} &= m_1(c_{12}c_{13})^2 + m_2 e^{-i\alpha_{21}}(s_{12}c_{13})^2 + m_3 e^{-i(\alpha_{31}-2\delta)}s_{13}^2 \\
m_{\mu\mu} &= m_1(s_{12}c_{23} + c_{12}s_{23}s_{13}e^{-i\delta})^2 + m_2 e^{-i\alpha_{21}}(c_{12}c_{23} - s_{12}s_{23}s_{13}e^{-i\delta})^2 + m_3 e^{-i\alpha_{31}}(s_{23}c_{13})^2 \\
m_{\tau\tau} &= m_1(s_{12}s_{23} - c_{12}c_{23}s_{13}e^{-i\delta})^2 + m_2 e^{-i\alpha_{21}}(c_{12}s_{23} + s_{12}c_{23}s_{13}e^{-i\delta})^2 + m_3 e^{-i\alpha_{31}}(c_{23}c_{13})^2 \\
m_{e\mu} &= -m_1 c_{12}c_{13}(s_{12}c_{23} + c_{12}s_{23}s_{13}e^{-i\delta}) + m_2 e^{-i\alpha_{21}} s_{12}c_{13}(c_{12}c_{23} - s_{12}s_{23}s_{13}e^{-i\delta}) \\
&\quad + m_3 e^{-i(\alpha_{31}-\delta)} s_{23}s_{13}c_{13} \\
m_{e\tau} &= m_1 c_{12}c_{13}(s_{12}s_{23} - c_{12}c_{23}s_{13}e^{-i\delta}) - m_2 e^{-i\alpha_{21}} s_{12}c_{13}(c_{12}s_{23} + s_{12}c_{23}s_{13}e^{-i\delta}) \\
&\quad + m_3 e^{-i(\alpha_{31}-\delta)} c_{23}s_{13}c_{13} \\
m_{\mu\tau} &= -m_1(s_{12}c_{23} + c_{12}s_{23}s_{13}e^{-i\delta})(s_{12}s_{23} - c_{12}c_{23}s_{13}e^{-i\delta}) \\
&\quad - m_2 e^{-i\alpha_{21}}(c_{12}c_{23} - s_{12}s_{23}s_{13}e^{-i\delta})(c_{12}s_{23} + s_{12}c_{23}s_{13}e^{-i\delta}) \\
&\quad + m_3 e^{-i\alpha_{31}} s_{23}c_{23}c_{13}^2 \,.
\end{aligned} \tag{13}$$

As known that the neutrino experiments can only measure the mass squared difference between different neutrino species denoted by $\Delta m_{ij}^2 = m_i^2 - m_j^2$. Since the sign of m_{31}^2 and the absolute masses of neutrinos cannot be determined, this leads to three possible mass spectra in the literature and they are: [1]

(1) normal ordering (NO) ($m_1 < m_2 < m_3$) with masses

$$m_{2(3)} = (m_1^2 + \Delta m_{21(31)}^2)^{1/2}\,; \tag{14}$$

(2) inverted ordering (IO) ($m_3 < m_1 < m_2$) with masses

$$m_1 = (m_3^2 + \Delta m_{13}^2)^{1/2}\,,\ m_2 = (m_1^2 + \Delta m_{21}^2)^{1/2}\,; \tag{15}$$

(3) quasi-degeneracy (QD)

$$m_1 \simeq m_2 \simeq m_3 = m_0,\ m_0 > 0.1 \text{ eV}. \tag{16}$$

Because the $m_{\ell'\ell}$ in Eq. (13) depends on the masses of neutrinos, the different mass patterns will lead to different patterns of Yukawa couplings. Consequently, the branching fractions for (δ^{++}, δ^{+}, δ^{0}) decaying to leptons are also governed by the mass patterns. We will explore their influence on the production of cosmic rays in DM annihilation.

C. Scalar Potential

In the considered model, one new odd doublet and one new triplet are included. Therefore, the new scalar potential with the Z_2-parity is given by

$$\begin{aligned} V(H,\Phi,\Delta) &= \mu^2 H^\dagger H + \lambda_1 (H^\dagger H)^2 + m_\Phi^2 \Phi^\dagger\Phi + \lambda_2 (\Phi^\dagger\Phi)^2 + \lambda_3 H^\dagger H \Phi^\dagger\Phi + \lambda_4 H^\dagger\Phi\Phi^\dagger H \\ &+ \frac{\lambda_5}{2}\left[(H^\dagger\Phi)^2 + h.c.\right] + m_\Delta^2 Tr\Delta^\dagger\Delta + \mu_1\left(H^T i\tau_2\Delta^\dagger H + h.c.\right) + \mu_2\left(\Phi^T i\tau_2\Delta^\dagger\Phi\right) \\ &+ \lambda_6 H^\dagger H Tr\Delta^\dagger\Delta + \bar{\lambda}_6\Phi^\dagger\Phi Tr\Delta^\dagger\Delta + \lambda_7 H^\dagger\Delta\Delta^\dagger H + \bar{\lambda}_7\Phi^\dagger\Delta\Delta^\dagger\Phi + \lambda_8 H^\dagger\Delta^\dagger\Delta H \\ &+ \bar{\lambda}_8\Phi^\dagger\Delta^\dagger\Delta\Phi + \lambda_9 (Tr\Delta^\dagger\Delta)^2 + \lambda_{10} Tr(\Delta^\dagger\Delta)^2 . \end{aligned} \tag{17}$$

Since the CP related issue is not discussed in this paper, all parameters are assumed to be real. Besides the SM parameters μ^2 and λ_1, there involve sixteen more free parameters. Since the SM Higgs doublet still dictates the electroweak symmetry breaking (EWSB), $\mu^2 < 0$ is required. The triplet and odd doublet have obtained their masses before EWSB, therefore we set $m_\Phi^2(m_\Delta^2) > 0$ and their values could be decided by the masses of odd (triplet) particles. We will see this point clearly later.

When H and Δ develop the VEVs, the scalar potential as a function of v_0 and v_Δ is found as

$$V(v_0, 0, v_\Delta) = \frac{\mu^2}{2}v_0^2 + \frac{\lambda_1}{4}v_0^4 + \frac{m_\Delta^2}{2}v_\Delta^2 + \frac{\lambda_6+\lambda_7}{4}v_0^2 v_\Delta^2 + \frac{\lambda_9+\lambda_{10}}{4}v_\Delta^4 - \frac{\mu_1}{\sqrt{2}}v_0^2 v_\Delta . \tag{18}$$

By using the minimal conditions of $\partial V/\partial v_0 = 0$ and $\partial V/\partial v_\Delta = 0$, we easily get

$$v_0 \approx \sqrt{\frac{-\mu^2}{\lambda_1}}, v_\Delta \approx \frac{\mu_1 v_0^2}{\sqrt{2}\left(m_\Delta^2 + \frac{\lambda_6+\lambda_7}{2}v_0^2\right)}, \tag{19}$$

where the condition of $v_\Delta \ll v_0$ has been used. From the results, we see that μ_1 is proportional to v_Δ. In the scheme of $\mu_1 \sim v_\Delta < 10^{-4}$ GeV, the associated effects in DM annihilation could be ignored.

According to Eq. (17), we can obtain the masses of new scalars and triple (quadratic) interactions of odd particles and triplet particles. We first discuss the masses of new scalar particles. For odd particles, if the small v_Δ effects are ignored, we find that the masses of $(S, A, H^\pm)$ are the same as those in the IHD model [24, 25] and given by

$$m_S^2 = m_\Phi^2 + \lambda_L v_0^2\,,\ m_A^2 - m_S^2 = -\lambda_5 v_0^2\,,\ m_{H^\pm}^2 = m_\Phi^2 + \frac{\lambda_3}{2} v_0^2 \tag{20}$$

with $\lambda_L = (\lambda_3 + \lambda_4 + \lambda_5)/2$. For SM Higgs and triplet particles, although the mixture of H and Δ could arise from triple coupling μ_1 term and quadratic terms, however, they are all related to v_Δ and μ_1. Due to $\mu_1 \sim v_\Delta$, the mixing effects could be neglected. For illustrating the small mixing effect, we take $G^0 - \eta^0$ as the example. According to Eq. (17), the mass matrix for $G^0 - \eta^0$ is given by

$$M_{G^0\eta^0} = \begin{pmatrix} \mu^2 + \lambda_1 v_0^2 + \sqrt{2}\mu_1 v_\Delta + \frac{\lambda_6}{4} v_\Delta^2 & \sqrt{2}\mu_1 v_0 \\ \sqrt{2}\mu_1 v_0 & m_\Delta^2 + \frac{\lambda_6+\lambda_7}{2} v_0^2 + v_\Delta^2(\lambda_9 + \lambda_{10}) \end{pmatrix}. \tag{21}$$

If we take $\mu_1, v_\Delta \ll v_0$, the mixing angle of G^0 and η^0 is $\theta_{G^0\eta^0} \sim 2v_\Delta/v_0 \ll 1$. With Eq. (19) and ignoring the small effects, we get

$$\begin{aligned} m_{G^0}^2 &\approx \mu^2 + \lambda_1 v_0^2 \approx 0\,, \\ m_{\eta^0}^2 &\approx m_\Delta^2 + \frac{\lambda_6 + \lambda_7}{2} v_0^2\,. \end{aligned} \tag{22}$$

Similarly, other scalar mixings are also small and negligible. Consequently, the masses of SM Higgs and triplet particles are given by

$$\begin{aligned} m_h^2 &\approx 2\lambda_1 v_0^2\,, m_{\delta^0}^2 \approx m_{\eta^0}^2 \approx m_\Delta^2 + \frac{\lambda_6 + \lambda_7}{2} v_0^2\,, \\ m_{\delta^{++}}^2 &\approx m_\Delta^2 + \frac{\lambda_6 + \lambda_8}{2} v_0^2\,, \\ m_{\delta^+}^2 &\approx \frac{1}{2}(m_{\delta^{++}}^2 + m_{\delta^0}^2)\,. \end{aligned} \tag{23}$$

We see that $m_{\delta^0} \approx m_{\eta^0}$ and m_{δ^+} is fixed when m_{δ^0} and $m_{\delta^{++}}$ are determined. We point out that the vertices from $\Phi^T i\sigma_2 \Delta^\dagger \Phi$ term are associated with a dimensional parameter μ_2. Unlike μ_1 which is limited to be much smaller than v_0, the value of μ_2 could be as large as few hundred GeV. It will have an interesting contributions to the cosmic-ray flux of neutrino from DM annihilation. We will further discuss its effects later.

Now we discuss the triple and quadratic interactions of scalar particles that are responsible for relic density and production of cosmic rays. According to Eq. (17), there appear lots

of new interactions among new scalar particles. However, for explaining the measured relic density and studying the excess of cosmic rays by the DM (co)annihilation, here we display those relevant interactions in Table I. In the table, we have ignored the couplings related to v_Δ and μ_1.

TABLE I: Triple and quadratic couplings of Z_2-odd and -even scalar particles for relic density and the excess of cosmic rays.

Vertex	Coupling	Vertex	Coupling
SSh	$2\lambda_L v_0$	AAh	$(\lambda_3+\lambda_4-\lambda_5)v_0$
$SS(AA)\delta^0$	$\mp\sqrt{2}\mu_2$	$SA\eta^0$	$-\sqrt{2}\mu_2$
$SH^\mp\delta^\pm$	$-\mu_2$	$AH^\mp\delta^\pm$	$\pm i\mu_2$
H^+H^-h	$\lambda_3 v_0$	$H^\pm H^\pm\delta^{\mp\mp}$	$2\mu_2$
$\delta^+\delta^-h$	$(\lambda_6+(\lambda_7+\lambda_8)/2)v_0$	$\delta^{++}\delta^{--}h$	$(\lambda_6+\lambda_8)v_0$
$\delta^0\delta^0(\eta^0\eta^0)h$	$(\lambda_6+\lambda_7)v_0$	hhh	$6\lambda_1 v_0$
$SS(H^+H^-)hh$	$2\lambda_L(\lambda_3)$	$AAhh$	$\lambda_3+\lambda_4-\lambda_5$
$SS(AA)\delta^+\delta^-$	$\bar\lambda_6+(\bar\lambda_7+\bar\lambda_8)/2$	$(S^2,A^2)\delta^0\delta^0[\eta^0\eta^0]$	$\bar\lambda_6+\bar\lambda_7$
$SS(AA)\delta^{++}\delta^{--}$	$\bar\lambda_6+\bar\lambda_8$	$H^+H^-\delta^+\delta^-$	$\bar\lambda_6+(\bar\lambda_7+\bar\lambda_8)/2$
$H^+H^-\delta^{++}\delta^{--}$	$\bar\lambda_6+\bar\lambda_7$	$H^+H^-\delta^0\delta^0(\eta^0\eta^0)$	$\bar\lambda_6+\bar\lambda_8$
$SH^-\delta^-\delta^{++}(H^+\delta^+\delta^{--})$	$-(\bar\lambda_7-\bar\lambda_8)/2$	$AH^+\delta^+\delta^{--}(H^-\delta^-\delta^{++})$	$\pm i/2(\bar\lambda_7-\bar\lambda_8)$
$SH^\mp\delta^\pm\delta^0$	$(\bar\lambda_7-\bar\lambda_8)/(2\sqrt{2})$	$AH^\mp\delta^\pm\eta^0$	$(\bar\lambda_7-\bar\lambda_8)/(2\sqrt{2})$
$SH^\pm\delta^\mp\eta^0$	$\pm i/(2\sqrt{2})(\bar\lambda_7-\bar\lambda_8)$	$AH^\mp\delta^\pm\delta^0$	$\pm i/(2\sqrt{2})(\bar\lambda_7-\bar\lambda_8)$

III. SETTING PARAMETERS AND BRANCHING FRACTIONS OF TRIPLET DECAYS

In the model, there involve many new free parameters and some of them are not independent. Since we are interested in the mass dependence, we will take the masses as the variables. Hence, the set of new independent free parameters can be chosen as follows:

$$\{m_S^2, m_A^2, m_{H^\pm}^2, \lambda_2, \lambda_L, m_{\delta^0}^2, m_{\delta^{\pm\pm}}^2, \mu_2, \lambda_6, \xi_A, \bar\lambda_6, \chi_A, \chi_B, \lambda_9, \lambda_{10}\} \tag{24}$$

with $\xi_{A(B)} = \lambda_6 + \lambda_{8(7)}$ and $\chi_{A(B)} = \bar{\lambda}_6 + \bar{\lambda}_{8(7)}$. Accordingly, the decided parameters are expressed as

$$\begin{aligned}
m_\Phi^2 &= m_S^2 - \lambda_L v_0^2\,,\ \lambda_3 = \frac{2}{v_0^2}\left(m_{H^\pm}^2 - m_\Phi^2\right)\,,\\
\lambda_5 &= \frac{m_S^2 - m_A^2}{v_0^2}\,,\ \lambda_4 = 2\lambda_L - \lambda_3 - \lambda_5\,,\\
m_\Delta^2 &= m_{\delta^{\pm\pm}}^2 - \frac{\xi_A}{2}v_0^2\,,\ \xi_B = \frac{2}{v_0^2}\left(m_{\delta^0}^2 - m_\Delta^2\right)\,,\\
\lambda_7 &= \xi_B - \lambda_6\,,\ \lambda_8 = \xi_A - \lambda_6\,,\\
\bar{\lambda}_7 &= \chi_A - \bar{\lambda}_6\,,\ \bar{\lambda}_8 = \chi_B - \bar{\lambda}_6\,.
\end{aligned} \tag{25}$$

In our approach, we choose the lightest odd particle (LOP) to be S, the DM candidate. For revealing the triplet contributions to the production of cosmic rays and relic density of DM, we suppress the effects from the original IHD model by assuming $\lambda_L = 0$ and the mass differences of odd particles being within few GeV, where the former leads the vertex of Higgs-$SS(AA)$ to vanish and the latter inhibits the (co)annihilation processes induced by gauge interactions. Therefore, for simplifying our numerical analysis, the values of free parameters are adopted as follows:

$$\begin{aligned}
\lambda_L = 0\,,\ m_S &= m_A - 1\ \text{GeV}\,, m_{H^\pm} = m_A\,,\\
m_{\delta^{\pm\pm}} &= m_{\delta^\pm} = m_{\delta^0} \equiv m_\delta = 500\ \text{GeV}\,.
\end{aligned} \tag{26}$$

Due to the mass degeneracy in triplet particles, i.e. $\lambda_6 + \lambda_{7(8)} = 0$, the interactions of $(\delta^{++}\delta^{--}, \delta^+\delta^-, \delta^0\delta^0, \eta^0\eta^0)h$ in Table I also vanish.

The new source to produce the positrons and neutrinos in the model is by the decays of triplet particles, where the main effects are associated with Yukawa couplings. As mentioned in Sec. II B, although the Yukawa couplings have been constrained by neutrino experiments, however the neutrino mass spectrum, Dirac phase and Majorana phases are still uncertain. For numerical analysis, we study three possible mass spectra defined in Eqs. (14)-(16) by taking $\delta = 0$ and $\phi_{21(31)} = 0$. For comparison, we also take $\delta = \phi_{31} = 0$ and $\phi_{21} = 1.7$ for QD to illustrate the influence of Majorana phase. Therefore, we use QDI and QDII to show the differences.

Numerically, we use the measured central values for the mixing angles (θ_{ij}) of PMNS matrix and for the mass squared differences, i.e. the inputs are taken as $\sin^2(2\theta_{12}) = 0.857$, $\sin^2(2\theta_{23}) = 0.95$, $\sin^2(2\theta_{13}) = 0.095$, $m_{12}^2 = 7.5 \times 10^{-5}$ eV and $|m_{31}^2| = 2.32 \times 10^{-3}$ eV.

For QD case, we set $m_0 = 0.2$ eV. As a result, the numerical values of $m_{\ell'\ell}$ in Eq. (13) are given in Table II. Since we have taken $v_\Delta < 10^{-4}$ GeV, triplet particles mainly decay to leptons. Hence, the corresponding branching ratios (BRs) for triplet decays are shown in Table III. The values in brackets in Table III are the BRs for $\delta^\pm$ decays. The difference between $\delta^{\pm\pm}(\delta^0, \eta^0)$ and $\delta^\pm$ is because the former has two identical particles in the final state; therefore, a proper symmetry factor has to be included.

TABLE II: Values of Yukawa couplings (in units of 10^{-2} eV) in NO, IO, QDI and QDII. The abbreviations could refer to the text.

	m_{ee}	$m_{e\mu}$	$m_{e\tau}$	$m_{\mu\mu}$	$m_{\mu\tau}$	$m_{\tau\tau}$
NO	0.3	0.6	0.1	1.4	1.0	1.4
IO	1.5	0.7	-1.1	1.0	-1.3	1.6
QDI	14.2	0	0	12.1	-2.1	12.4
QDII	$10.3e^{-i0.4}$	$5.9e^{-i2.4}$	$7.9e^{i0.7}$	$8.8e^{-i0.4}$	$5.8e^{i0.1}$	$8.2e^{-i0.9}$

TABLE III: Branching ratios (BRs) for $\delta^{\pm\pm}(\delta^0, \eta^0)$ and $\delta^\pm$ decays in NO, IO, QDI and QDII where the corresponding values of Yukawa couplings are given in Table II. ℓ_f could be charged lepton or neutrino and it depends on what its parent is. The values in brackets denote the BRs for $\delta^\pm$ decays.

	$\ell_e\ell_e$	$\ell_e\ell_\mu$	$\ell_e\ell_\tau$	$\ell_\mu\ell_\mu$	$\ell_\mu\ell_\tau$	$\ell_\tau\ell_\tau$
NO	0.01 [0.02]	0.1 [0.06]	0[0]	0.3 [0.39]	0.29 [0.18]	0.28 [0.35]
IO	0.17 [0.23]	0.08 [0.06]	0.2 [0.14]	0.08 [0.11]	0.26 [0.17]	0.21[0.29]
QDI	0.39 [0.40]	0 [0]	0 [0]	0.29 [0.29]	0.02 [0]	0.30 [0.31]
QDII	0.21[0.28]	0.13[0.09]	0.24[0.16]	0.15[0.20]	0.13[0.09]	0.13[0.18]

IV. RELIC DENSITY AND FLUXES AND ENERGY SPECTRA OF COSMIC RAYS

After establishing our model and deciding the set of parameters, in this section we discuss the effects of new interactions on the relic density of DM and their implications on the

indirect DM detection experiments for cosmic rays. Since all odd particles belong to the IHD, the interesting (co)annihilation processes which determine the relic density of DM could be classified as three scenarios: (I) s-channel from quadratic couplings, (II) t-channel from triple couplings and (III) s-channel from triple couplings, where the initial states only involve IHD and the final states are triplet particles and leptons. The corresponding Feynman diagrams are shown in Fig. 1. The particles in initial and final states are decided by the couplings shown in Table I. Although $W^\pm$ and Z pairs could be generated by gauge interactions or by s-channel process mediated by SM-Higgs, due to the parameter setting in Eq. (26) and $m_\Phi \sim O(\text{TeV})$, their production cross sections by the (co)annihilation processes are secondary effects. We will ignore their contributions to relic density in our analysis.

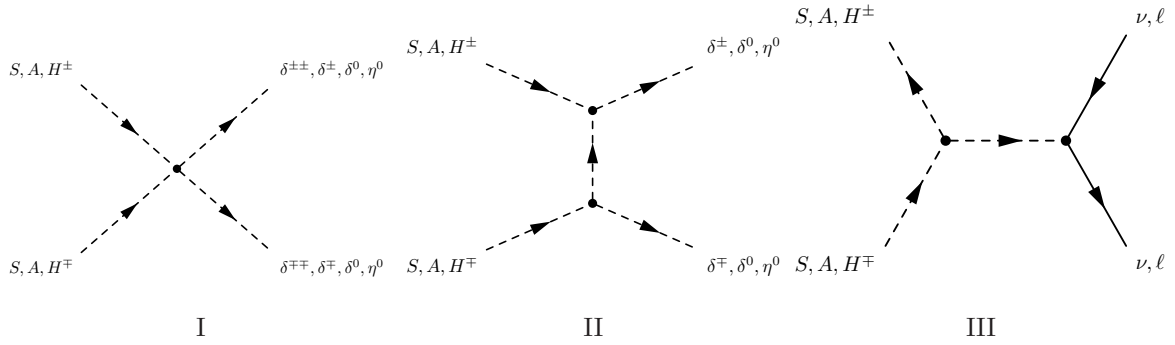

FIG. 1: Three scenarios of (co)annihilation processes of odd particles for relic density: (I) s-channel by quadratic interactions, (II) t-channel by triple interactions and (III) s-channel by triple interactions.

In terms of the set of parameters in Eq. (24) and the Yukawa couplings in Eq. (10), the scenarios I, II and III depend on the parameter sets $\{\chi_A, \chi_B\}$, $\{\mu_2\}$ and $\{\mu_2, h_{\ell'\ell}\}$, respectively. In addition, the two parameters χ_A and χ_B in scenario-I will result different energy spectra of positrons and neutrinos. For further studying their contributions, we therefore consider three schemes for scenario-I as follows : (I_a) $\chi_A \gg \chi_B \approx 0$, ($\text{I}_b$) $\chi_A = \chi_B$ and (I_c) $\chi_A \approx 0 \ll \chi_B$.

According to the taken values of parameters in Eq. (26) and Table II, the free parameters now are m_S, $\chi_{A,B}$, μ_2 and $h_{\ell'\ell}$. We note that because of $h_{\ell'\ell} = \sqrt{2} m_{\ell'\ell}/v_\Delta$, when the values of $m_{\ell'\ell}$ are fixed as shown in Table II, the associated free parameter of $h_{\ell'\ell}$ indeed is v_Δ. In our approach, we first constrain the free parameters so that the observed relic density of DM, Ωh^2, could be explained in our chosen scenarios. With the constrained parameters, we

then estimate the fluxes of cosmic-ray antiprotons, positrons, electrons and neutrinos. As mentioned earlier, for explaining the excess of the cosmic rays by DM annihilation, usually we need a BF. The BF could be arisen from several mechanisms, such as astrophysical origin [44], Sommerfeld enhancement [47], near-threshold resonance and dark-onium formation [48], etc. Since we do not focus on such effect in the model, as used in the literature we take it as an undetermined parameter and its value could be limited by the antiproton flux measured by AMS [32], PAMELA [33] and HESS [34]. With the decided BF, we study the positron/electron and neutrino fluxes in various situations of free parameters.

A. Relic Density

Now we start to make the numerical analysis for the Ωh^2 by DM S (co)annihilation processes. For numerical calculations, we implement our model to CalcHEP [49] and use `micrOMEGAs` [50] to estimate the Ωh^2. To constrain the parameters, we require the relic density of S to satisfy the 90% CL (confidence level) range of its experimental value, written as

$$0.1159 \leq \Omega h^2 \leq 0.1215\,. \tag{27}$$

In the following we individually discuss the contributions from scenario-I, -II and -III.

For scenario-I, as stated above, we classify three schemes based on the relative magnitude of parameters χ_A and χ_B. With the values of parameters in Eq. (26) and the range of Ωh^2 in Eq. (27), the correlation between m_S and $\chi_A(\chi_B)$ in scheme-$\mathrm{I}_{a(c)}$ is given in the left panel of Fig. 2. We find that the schemes I_a and I_c have the same contributions. Similarly, the results of scheme I_b are displayed in the right panel of Fig. 2. We see that $\chi_{A,B}$ of $O(1)$ can accommodate to the observed Ωh^2.

For scenario-II, the involved parameters are m_S and μ_2. Differing from other parameters, μ_2 is a mass dimension one parameter and its natural value could be from GeV to TeV. With the data of Ωh^2, we present the correlation between m_S and μ_2 in the left panel of Fig. 3. By the plot, we see that if the scenario-II is the only source of the observed Ωh^2, the value of μ_2 has to be as large as the scale of m_S.

For scenario-III, the related parameters are μ_2 and $h_{\ell'\ell}$. Thus, we expect that the limit on μ_2 with $m_\Delta < m_S$ should be similar to the cases in scenario-II. However, the more interest

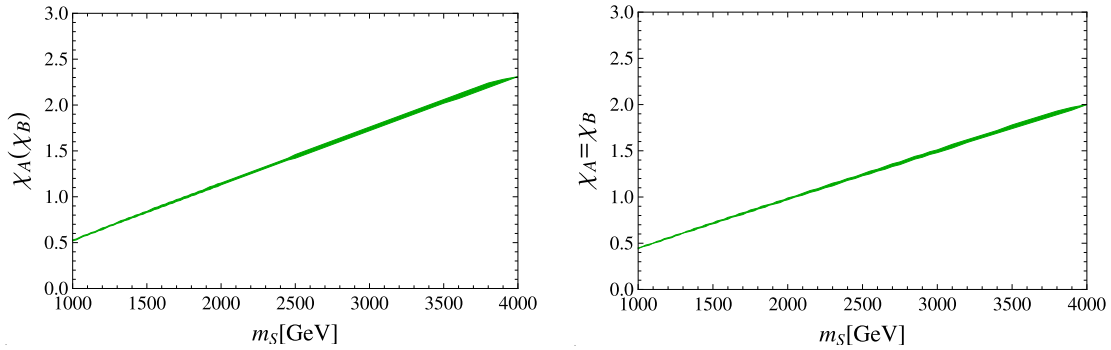

FIG. 2: The allowed region in scenario-I when Ωh^2 is satisfied. Left panel denotes the correlation between m_S and $\chi_A(\chi_B)$ in scheme $\mathrm{I}_{a(c)}$. Right panel stands for the results of scheme I_b. Schemes I_a and I_c have the same results.

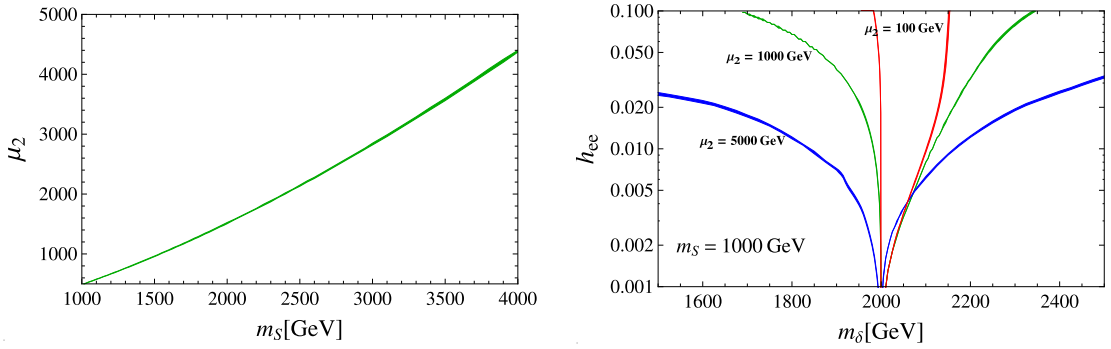

FIG. 3: The allowed region for scenario-II (left) and scenario-III (right). For scenario III, we plot the contours of Ωh^2 as a function of h_{ee} and m_Δ with various values of μ_2 and $m_S = 1000$ GeV.

of this scenario is the reverse case. From Fig. 1-III, we see that the intermediate state is triplet particle. When $m_\Delta \approx 2m_S$ is satisfied, we have a large effect from the Breit-Wigner enhancement. As discussed before, Yukawa couplings are determined by $h_{\ell'\ell} = \sqrt{2}m_{\ell'\ell}/v_\Delta$. If we use the fixed values in Table II, the free parameter is only v_Δ. Since we only need one parameter to describe all $h_{\ell'\ell}$, here we just take h_{ee} as the representative. Once h_{ee} is determined, other $h_{\ell'\ell}$ are also fixed. Accordingly, we present the results as a function of h_{ee} and m_Δ with several values of μ_2 in the right panel of Fig. 3, where we only use the IO for neutrino mass spectrum and $m_S = 1000$ GeV as an illustration. We find that due to the Breit-Wigner enhancement, a smaller value of μ_2 could get desired magnitude of the (co)annihilation cross section.

B. Antiproton spectrum and boost factor constraint

As mentioned earlier, the necessary BF for explaining the excess of cosmic ray fluxes by DM annihilation is regarded as a parameter. However, the value of BF can not be arbitrary and we need to investigate the limit of BF by the observed data. It is known that cosmic-ray antiprotons have been measured by AMS [32], PAMELA [33] and BESS [34]. By the data, we see that below the energy of 100 GeV, the measurements fit well with the models of cosmic-ray background. Therefore, when the values of parameters are fixed by Ωh^2, antiproton flux $\Phi_{\bar{p}}$ could provide an upper limit on the BF.

In the model, since triplet particles only couple to leptons and cannot produce the antiprotons, the channels to generate antiprotons are from W and Z decays following WW and ZZ pair production, where WW and ZZ are produced from s-channel and t-channel by the gauge interactions $SS(AA)VV$ and $S(A)H^{\pm}W^{\mp}[SAZ]$ that are listed in Table I, respectively. We note that in our taken values of parameters, although the production of WW and ZZ for contributing to Ωh^2 is secondary effects, however it becomes the leading contributions to the antiproton production. Additionally, since the gauge coupling is known and fixed, m_S is the only free parameter for WW and ZZ production. Therefore, the limit on BF is clear.

For estimating $\Phi_{\bar{p}}$, we applied Navarro-Frenk-White (NFW) density profile for DM density distribution in the galactic halo [51]. For cosmic-ray antiproton background, we use the fitting function parametrized by [52]

$$log_{10}\Phi_{\bar{p}}^{\rm bkg} = -1.64 + 0.07x - x^2 - 0.02x^3 + 0.028x^4 \tag{28}$$

with $x = \log_{10}\mathrm{T/GeV}$, where the result is arisen from the analysis in Ref. [53]. Using `micrOMEGAs`, we present our results in Fig. 4, where the galactic propagation of charged particles and solar modulation effect are also taken into account. The left (right) panel of Fig. 4 shows the background and background+DM for $\Phi_{\bar{p}}$ in which $m_S = 1000(3000)$ GeV is used and various values of BF are taken. Since PAMELA [33] and AMS [32] results are more precise, we just show these data in the figure. We also use its data to constrain the BF. We find that the upper bound on the boost factor is $\sim 30(1800)$ for $m_S = 1000(3000)$ GeV. The upper value of BF with the corresponding value of m_S is given in Table IV. By the results, we see clearly that the new physics contributions have a significant deviation

from the background at $E > 100$ GeV. Therefore, the data at such energy region could test the model.

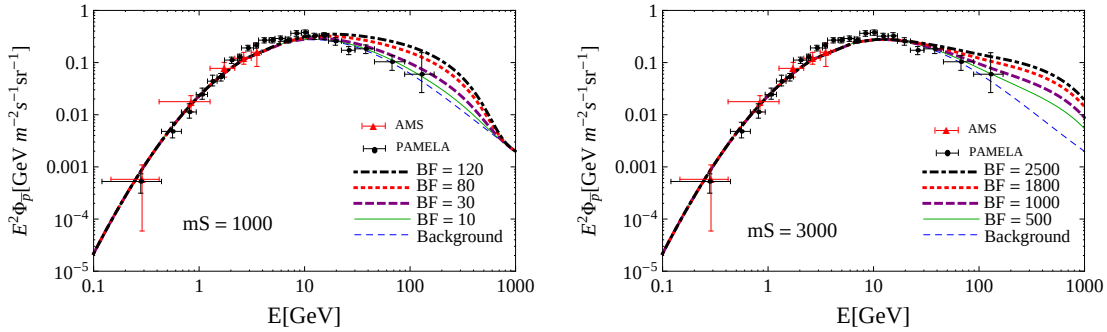

FIG. 4: Background and background + DM of cosmic-ray antiproton flux in different values of BF with $m_S = 1000$ GeV (left) and $m_S = 3000$ GeV (right). The data points stand for the PAMELA [33] and AMS [32] results.

TABLE IV: Upper bound of the BF for different values of m_S.

m_S [GeV]	1000	2000	3000	4000
BF	$\lesssim 30$	$\lesssim 500$	$\lesssim 1800$	$\lesssim 4500$

C. Cosmic-ray positron and electron spectra

After discussing the constraints of free parameters and the limit of the BF, we investigate the influence of DM annihilation on the positron/electron and neutrino fluxes. We first study the case for cosmic-ray positrons/electrons. Besides the new source for the fluxes of electron and positron, we also need to understand the background contributions of primary and secondary electrons and secondary positrons, in which the former comes from supernova remnants and the spallation of cosmic rays in the interstellar medium, respectively, while the latter could be generated by primary protons colliding with other nuclei in the interstellar medium. In our numerical calculations, we use the parametrizations, given by [54, 55]

$$\Phi_{e^-}^{\rm prim}(E) = \kappa \frac{0.16E^{-1.1}}{1+11E^{0.9}+3.2E^{2.15}} \quad [\mathrm{GeV}^{-1}\mathrm{cm}^{-2}\mathrm{s}^{-1}\mathrm{sr}^{-1}],$$
$$\Phi_{e^-}^{\rm sec}(E) = \frac{0.70E^{0.7}}{1+110E^{1.5}+600E^{2.9}+580E^{4.2}} \quad [\mathrm{GeV}^{-1}\mathrm{cm}^{-2}\mathrm{s}^{-1}\mathrm{sr}^{-1}],$$
$$\Phi_{e^+}^{\rm sec}(E) = \frac{4.5E^{0.7}}{1+650E^{2.3}+1500E^{4.2}} \quad [\mathrm{GeV}^{-1}\mathrm{cm}^{-2}\mathrm{s}^{-1}\mathrm{sr}^{-1}], \tag{29}$$

where $\Phi^{\rm prim(sec)}$ denotes the primary (secondary) cosmic ray. Accordingly, the total electron and positron fluxes are defined by

$$\begin{aligned}\Phi_{e^-} &= \kappa\Phi^{\rm prim}_{e^-} + \Phi^{\rm sec}_{e^-} + \Phi^{\rm DM}_{e^-}\,,\\ \Phi_{e^+} &= \Phi^{\rm sec}_{e^+} + \Phi^{\rm DM}_{e^+}\,,\end{aligned} \tag{30}$$

where $\Phi^{\rm DM}_{e^{-(+)}}$ is the electron(positron) flux from DM annihilations. According to Refs. [54] and [56], we have regarded the normalization of the primary electron flux to be undetermined and parametrized by the parameter of κ. In our analysis, we use $\kappa = 0.78$ to fit the experimental data for background.

When we study the relic density, we have used three scenarios to classify the parameters. Except the scenario-III that only can contribute to cosmic-ray neutrinos, the scenario-I and -II could be also applied to the cosmic-ray electrons and positrons by DM annihilation. Since the quadratic couplings of $SS\Delta\bar{\Delta}$ only depend on χ_A and χ_B, we could apply the schemes I_a, I_b and I_c, which have been constrained by relic density, to the production of cosmic-ray. Due to $v_\Delta < 10^{-4}$ GeV, the positron and electron production is dominated by $\delta^{\pm\pm}$ and $\delta^{\pm}$ decays. Since the BRs of triplet decaying to leptons have been given in Table III, in order to understand the cross section for producing the triplet pairs, we calculate the normalized cross section in each scenario and present the results in Table V, where the normalisation is defined by $\sigma(SS \to \delta_i\bar{\delta}_i)/\sum_i \sigma(SS \to \delta_i\bar{\delta}_i)$ with $\delta_i = \delta^{++}, \delta^{+}, \delta^0, \eta^0$.

TABLE V: Normalized cross section for DM annihilating to triplet-pair in each scenario.

channel	$\delta^{++}\delta^{--}$	$\delta^{+}\delta^{-}$	$\delta^0\delta^0$	$\eta^0\eta^0$
I_a	4/5	1/5	0	0
I_b	2/6	2/6	1/6	1/6
I_c	0	1/5	2/5	2/5
II	0	1/5	2/5	2/5

Combining the constraints of free parameters and the mass spectra of neutrinos discussed before, we now study the numerical analysis for cosmic-ray positron and electron spectra. First we focus on the positron/electron production via doubly charged scalar δ^{++}. The channel is interesting because not only it has a larger normalized cross section shown in Table V, but also there are six different modes to generate positrons/electrons, such as

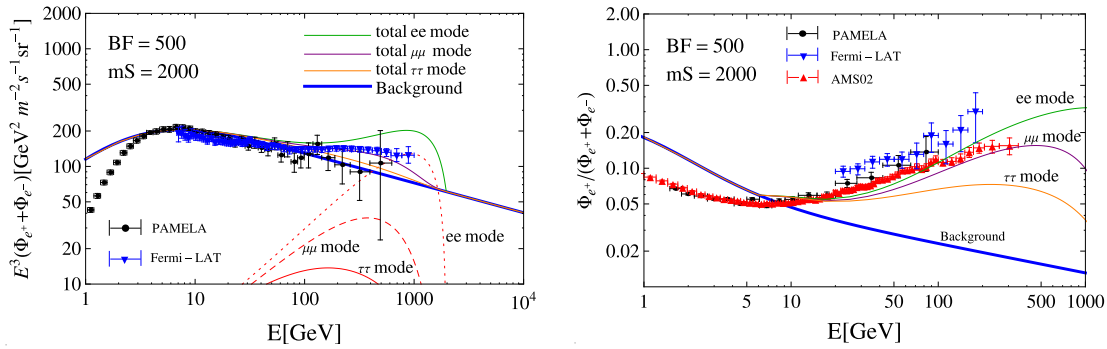

FIG. 5: The electron+positron spectra (left) and positron fraction (right) from $\delta^{\pm\pm} \to \ell^\pm\ell^\pm$ decays, where we adopt scenario-I$_a$ and NO for neutrino masses and take $m_S = 2000$ GeV and boost factor $BF = 500$. The associated experiments data are PAMELA [6, 8] and Fermi-LAT [7, 9] and AMS02 [5].

$\delta^{++} \to (e^+e^+, e^+\mu^+, e^+\tau^+, \mu^+\mu^+, \mu^+\tau^+, \tau^+\tau^+)$, where μ^+ and τ^+ then continue decaying to positron by the electroweak interactions in the SM. For demonstrating the behavior of multiple decay chains, we show $\Phi_{e^+} + \Phi_{e^-}$ and $\Phi_{e^+}/(\Phi_{e^+} + \Phi_{e^-})$ for the modes $\delta^{\pm\pm} \to \ell^\pm\ell^\pm$ with $\ell = e, \mu, \tau$ in Fig. 5, where for illustration, we choose the scheme I$_a$, NO for neutrino masses, $m_S = 2000$ GeV and $BF = 500$. For comparisons, we also show the data, measured by PAMELA [8] and Fermi-LAT [9] for $\Phi_{e^-} + \Phi_{e^+}$ and by PAMELA [6], Fermi-LAT [7] and AMS-02 [5] for $\Phi_{e^+}/(\Phi_{e^+} + \Phi_{e^-})$, in the figure. By the results, we clearly see that the curve for positron+electron spectrum from $\mu\mu$ mode is flatter than that from ee mode, and the spectrum from $\tau\tau$ mode is more flat and just slightly over the background. For $\Phi_{e^+}/(\Phi_{e^+} + \Phi_{e^-})$, $\tau\tau$ mode gives too small contribution to fit the measurements while ee and $\mu\mu$ are much close to the experimental data in the measured region.

In the following we discuss the fluxes of cosmic-ray positrons and electrons that are from all possible sources. First, in Table VI we present the required BFs for fitting the excess measured by PAMELA, Fermi-LAT and AMS-02. We see that the BFs for scenario-I$_c$ and -II have been over the upper bounds ($BF_{\rm max}$) that are obtained from antiproton measurement. In scenario-I$_a$ and -I$_b$, for satisfying the bound of BF, the mass of DM should be heavier than 1000 GeV. The values in brackets in the table denote the required BFs for neutrino masses with NO, IO, QDI and QDII by turns. It is found that the required BFs in scenarios I$_a$ and I$_b$ are close to each other.

We calculate $E^3(\Phi_{e^+} + \Phi_{e^-})$ and $\Phi_{e^+}/(\Phi_{e^+} + \Phi_{e^-})$ and show the results as a function of

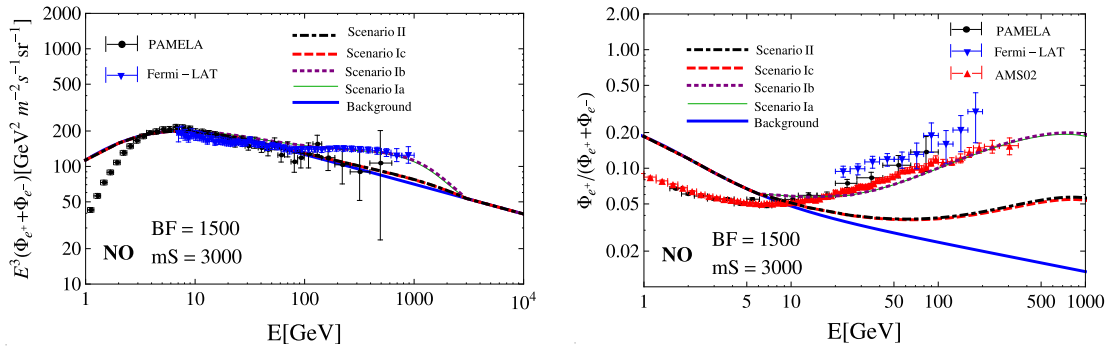

FIG. 6: The positron+electron spectrum (left) and positron fraction (right) for normal ordered neutrino masses, where we have used $m_S = 3000$ GeV and boost factor $BF = 1500$. The (solid, dotted, dashed, dot-dashed) line corresponds to scenario (I_a, I_b, I_c, II). The thick solid line is the cosmic-ray background. For left panel, we quote the data of PAMELA [8] and Fermi-LAT [9]. For right panel, we quote the data of PAMELA [6], Fermi-LAT [7] and AMS02 [5].

energy in Fig. 6, 7, 8 and 9 for neutrino masses with NO, IO, QDI and QDII, respectively, where we adopt $m_S = 3000$ GeV and $BF = 1500$, the solid, dotted, dashed and dash-dotted lines in turn denote the scenario-I_a, -I_b, -I_c and -II. The thick solid line is the cosmic-ray background in Eq. (29). We see that the contributions of scenario-I_c and scenario-II are much smaller than the data. According to the results in Figs. 6-9, we conclude that different neutrino mass spectrum could cause slight difference in positron/electron flux. Nevertheless, the normal ordered mass spectrum has a better matching with current data. We note that positron/electron flux in higher energy region tends to be larger when $BR(\Delta \to \ell_e \ell_e)$ is

TABLE VI: Required BF in each scenario associated with m_S for explaining positron/electron excess, where $BF > BF_{\rm max}$ indicates the necessary BF over the upper limit of antiproton flux. The values in brackets stand for the required BFs for neutrino masses with NO, IO, QDI and QDII by turns.

m_S	1000 GeV	2000 GeV	3000 GeV	4000 GeV
I_a	$BF > BF_{\rm max}$	(500, 500, 500, 500)	(1400, 1200, 900, 1100)	(2000, 1900, 1500, 1900)
I_b	$BF > BF_{\rm max}$	(500, 500, 500, 500)	(1400, 1200, 900, 1200)	(2000, 1900, 1500, 1800)
I_c	$BF > BF_{\rm max}$	$BF > BF_{\rm max}$	$BF > BF_{\rm max}$	$BF > BF_{\rm max}$
II	$BF > BF_{\rm max}$	$BF > BF_{\rm max}$	$BF > BF_{\rm max}$	$BF > BF_{\rm max}$

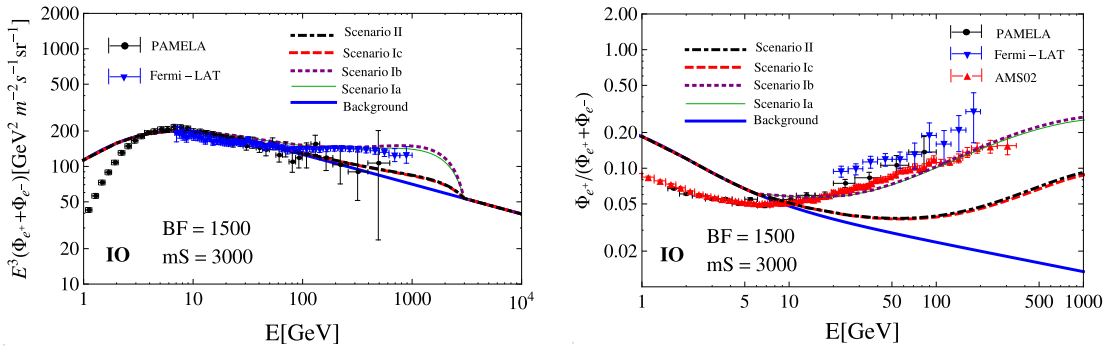

FIG. 7: The legend is the same as Fig. 6 but for inverted neutrino masses.

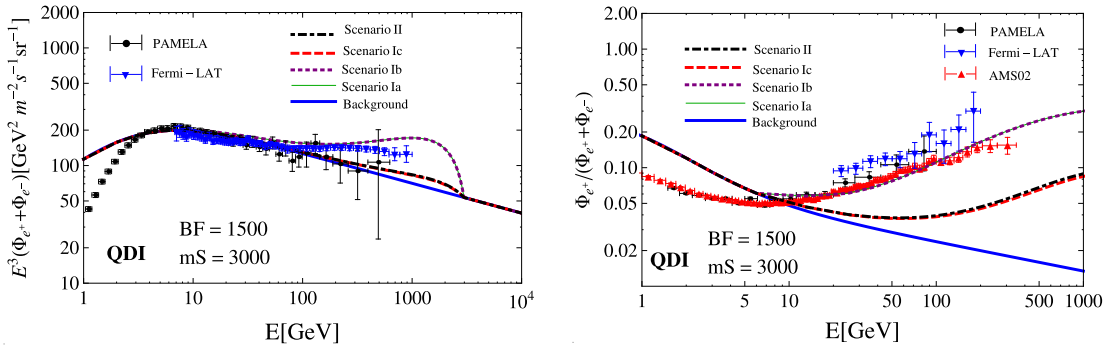

FIG. 8: The legend is the same as Fig. 6 but for QDI.

larger. In Fig. 10, we also show $E^3(\Phi_{e^+}+\Phi_{e^-})$ and $\Phi_{e^+}/(\Phi_{e^+}+\Phi_{e^-})$ for $m_S = 1000$, 2000, 3000 and 4000 GeV in scenario-I_a with NO and $BF = 1500$. We can see that the end point of positron fraction excess corresponds to the mass of DM. Thus, the measurement of the positron fraction in higher energy region is important to test the model and tell us the mass of DM.

D. Cosmic-ray neutrinos

As known that the necessary BF in scenario-I_c and -II for explaining the positron excess has been excluded by the data of antiproton spectrum, in the following we focus on scenario-$I_{a,b}$ and -III for cosmic-ray neutrinos induced by DM annihilation of galactic halo. For scenario-$I_{a,b}$, the cosmic-ray neutrinos are arisen from the decays of $\delta^{\pm}$, δ^0 and η^0. As known that the original neutrino species from DM annihilation can not be distinguished by experiments, we sum over all possible neutrino final states. It is expected that the results are independent of the Yukawa couplings in $\Delta \to \nu_i \nu_j$ decays, i.e. independence of neutrino mass spectrum. However, the involved parameters for triplet production are the same as those in

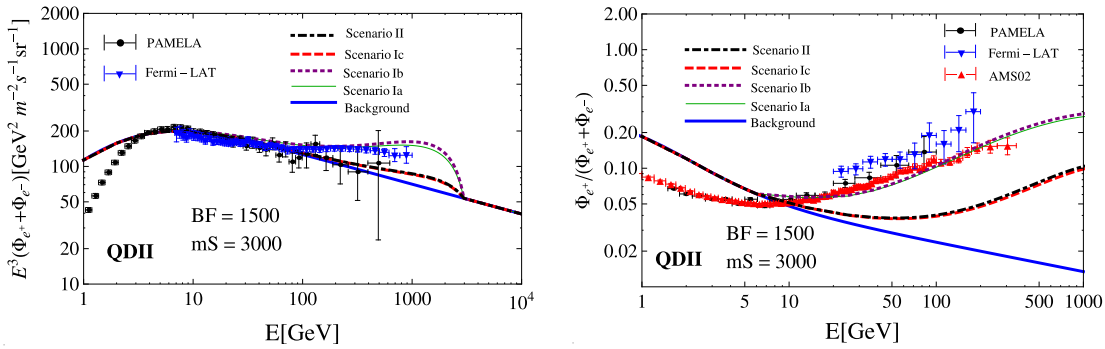

FIG. 9: The legend is the same as Fig. 6 but for QDII.

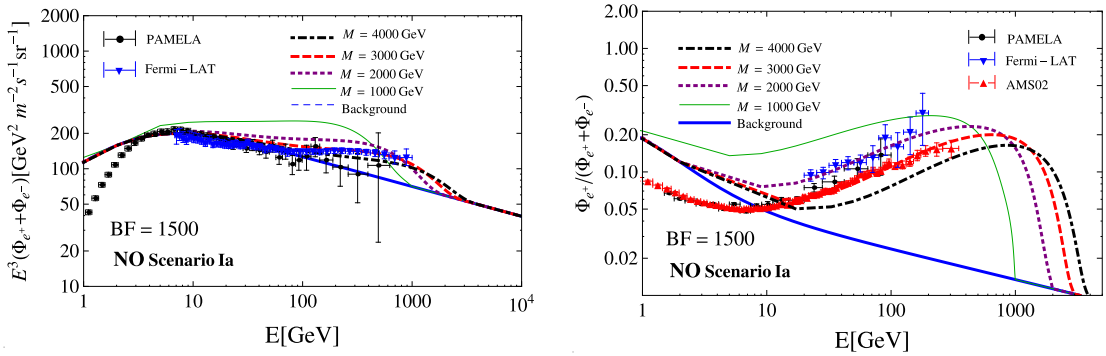

FIG. 10: The positron+electron spectrum (left) and positron fraction (right) for normal ordered neutrino masses, where we have used m_S = 1000, 2000, 3000 and 4000 GeV and boost factor $BF = 1500$. The experimental data are the same as those in Figs. 6-9.

the study of positron flux, where we have required different BFs in different neutrino mass spectra. Due to the reason, the neutrino production rates in our calculations still depend on the neutrino mass spectra. Hence, with the values of BF in Table VI and with the same values of free parameters for fitting positron/electron flux, we compute the velocity-averaged cross section paired triplet production for each scenario and present the results in Fig. 11, where we have used the sum defined by

$$\langle\sigma v\rangle = \langle\sigma v\rangle_{SS\to\delta^+\delta^-} + 2\langle\sigma v\rangle_{SS\to\delta^0\delta^0} + 2\langle\sigma v\rangle_{SS\to\eta^0\eta^0}\,. \tag{31}$$

The factor 2 in second and third terms is due to doubled neutrino flux from $\delta^0(\eta^0)$ decays. In the figure, we also show the upper limit of IceCube neutrino flux data for galactic halo, which are indicated from W^+W^- and $\mu^+\mu^-$ pairs [45, 46]. We clearly see that although both results of I_a and I_b are lower than the upper bound of data, the scenario-I_a is much close to the bound. The IceCube measurement will give a further limit on our parameters when more observational data are analysed.

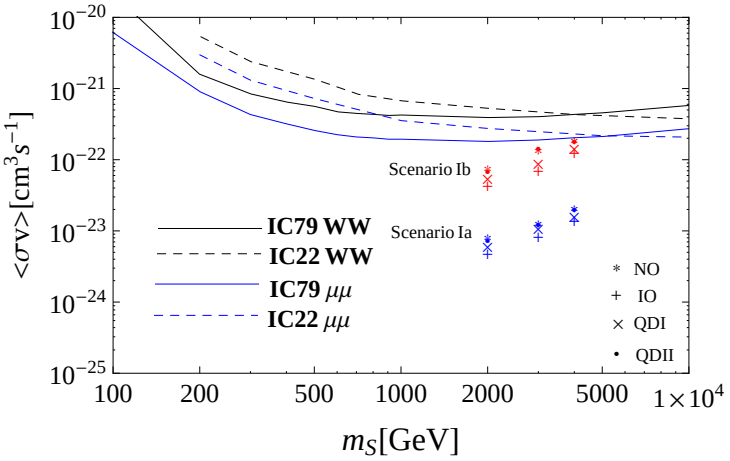

FIG. 11: Velocity-average cross section, $\langle\sigma v\rangle$, annihilating into triplet pairs for neutrino production in scenario-I_a and I_b with different neutrino mass spectra. The solid and dashed lines stand for the upper limit of IceCube-22 [45] and IceCube-79 [46] by assuming DM annihilating into W^+W^- and $\mu^+\mu^-$.

For scenario-III, it is known that when we study the relic density, a Breit-Wigner enhancement appears at $m_\Delta \approx 2m_S$. It is interesting to investigate the scenario for cosmic-ray neutrinos when the same enhancement occurs. Unlike the cases in I_a and I_b in which triplet particles are on-shell, the intermediate state δ^0 in scenario-III could be off-shell, i.e. the dependence of $h_{\ell'\ell}$ cannot be removed. Additionally, due to the resonant effect which leads to $\langle\sigma v\rangle \propto 1/v^4$ for small width of mediating particle, we find that a large neutrino flux is obtained without BF. Like the case in relic density, we still use h_{ee} as the free parameter for $h_{\ell'\ell}$ and its constraint could refer to the Fig. 3. By taking $m_\Delta = 2m_S(1-\epsilon)$ and with the values of parameters constrained by the DM relic density, $\langle\sigma v\rangle$ for $SS \to \nu\nu(\bar{\nu}\bar{\nu})$ as a function of m_S with several values of ϵ is displayed in Fig. 12, where the left (right) panel is for $\mu_2 = 1000(100)$ GeV. The solid and dashed line denotes the IceCube upper limit with 79-string [46] and 22-string [45], respectively. We note that for $\mu_2 = 100$ GeV, the region $m_S \gtrsim 2600$ GeV can not explain the relic density even if there is a Breit-Wigner enhancement. By the figure, we see that the current IceCube data could limit the value of ϵ. We expect that with more data analysis, IceCube could further limit the free parameters of scenario-III.

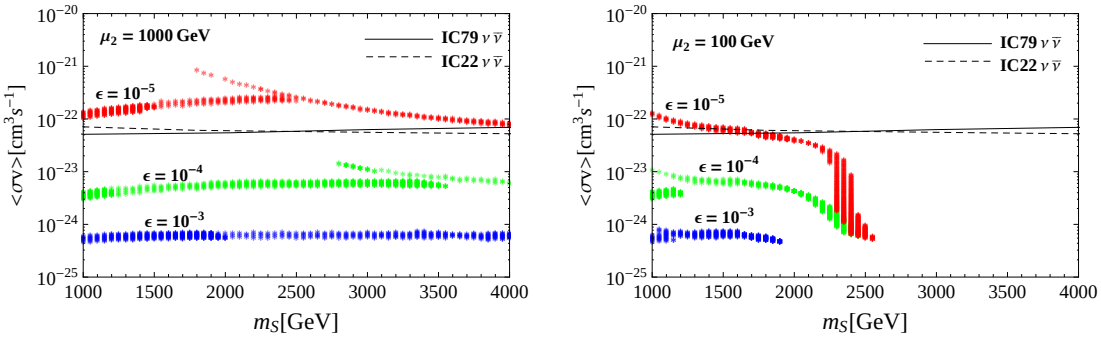

FIG. 12: $\langle\sigma v\rangle$ for $SS \to \nu\nu(\bar{\nu}\bar{\nu})$ as a function of m_S with selected values of ϵ. The left(right) panel is for $\mu_2 = 1000(100)$ GeV. The solid and dashed line stands for the IceCube upper limit with 79-string [46] and 22-string [45], respectively.

V. SUMMARY

For explaining the measured positron excess by the DM annihilation, we have studied the extension of the SM by adding an odd IHD Φ and an even Higgs triplet Δ. The LOP of Φ can be a WIMP DM candidate. Due to the unbroken Z_2-parity, the DM candidate is stable. We take the CP-even component S as the DM candidate. The neutrinos become massive through the type-II seesaw mechanism.

In order to suppress the effects from IHD model and emerge the triplet contributions, we have set $\lambda_L = 0$, $m_A - m_S = 1$ GeV and $m_{H^\pm} = m_A$. Even though, the antiproton spectrum is dominated by triple interactions $SH^\pm W^\mp$ and SAZ and quadratic interactions $SS(W^\pm W^\mp, ZZ)$ which appear in IHD model. With the measurement of antiproton spectrum, we study the correlation between the upper bound of BF and m_S.

In terms of the Feynman diagrams, three scenarios are involved in our analysis. In scenario-I, we further use three schemes to describe the parameters χ_A and χ_B. In our model, the excess of positrons/electrons is mainly arisen from the triplet decays. Since the neutrino mass spectrum is still uncertain, we also study the influence of neutrino mass in the cases of NO, IO and QD. From Figs. 6-9, we see that scenario-I$_a$ and -I$_b$ have similar contributions. Moreover, the normal ordered mass spectrum could fit well to the excess of positrons/electron measured by PAMELA, Fermi-LAT and AMS-02.

Although we have not observed the excess of comic-ray neutrinos, however if the source of excess of positrons/electrons is from triplet decays, the same effects will also increase the abundance of cosmic-ray neutrinos. We find that the quasi-resonance effects at $m_\Delta \approx 2m_S$

could occur in scenario-III so that large neutrino flux can be obtained without BF. We calculate $\langle \sigma v \rangle$ for cosmic-ray neutrinos and realize that our results in some parameter region are close to the recent IceCube data for neutrino flux from galactic halo. Hence, our model could be tested if more data for cosmic-ray neutrinos are observed.

Acknowledgments

We thank Dr. A. Pukhov for providing the revised code of micrOMEGAs. This work is supported by the National Science Council of R.O.C. under Grant #: NSC-100-2112-M-006-014-MY3 (CHC) and NSC-102-2811-M-006-035 (TN). We also thank the National Center for Theoretical Sciences (NCTS) for supporting the useful facilities.

[1] J. Beringer *et al.* (Particle Data Group), Phys. Rev. D**86**, 010001 (2012).

[2] P. A. R. Ade *et al.* [Planck Collaboration], arXiv:1303.5062 [astro-ph.CO].

[3] D.S. Akerib *et al.* [LUX Collaboration], arXiv:1310.8214 [astro-ph.CO].

[4] E. Aprile *et al.* [XENON100 Collaboration], Phys. Rev. Lett. **109**, 181301 (2012) [arXiv:1207.5988 [astro-ph.CO]].

[5] M. Aguilar *et al.* [AMS Collaboration], Phys. Rev. Lett. **110**, no. 14, 141102 (2013).

[6] O. Adriani *et al.* [PAMELA Collaboration], Nature **458**, 607 (2009) [arXiv:0810.4995 [astro-ph]].

[7] M. Ackermann *et al.* [Fermi LAT Collaboration], Phys. Rev. Lett. **108**, 011103 (2012) [arXiv:1109.0521 [astro-ph.HE]].

[8] O. Adriani *et al.* [PAMELA Collaboration], Phys. Rev. Lett. **106**, 201101 (2011) [arXiv:1103.2880 [astro-ph.HE]].

[9] M. Ackermann *et al.* [Fermi LAT Collaboration], Phys. Rev. D **82**, 092004 (2010) [arXiv:1008.3999 [astro-ph.HE]].

[10] J. Chang, J. H. Adams, H. S. Ahn, G. L. Bashindzhagyan, M. Christl, O. Ganel, T. G. Guzik and J. Isbert *et al.*, Nature **456**, 362 (2008).

[11] F. Aharonian *et al.* [H.E.S.S. Collaboration], Phys. Rev. Lett. **101**, 261104 (2008) [arXiv:0811.3894 [astro-ph]].

[12] F. Aharonian *et al.* [H.E.S.S. Collaboration], Astron. Astrophys. **508**, 561 (2009)

[arXiv:0905.0105 [astro-ph.HE]].

[13] D. Hooper, P. Blasi and P. D. Serpico, JCAP **0901**, 025 (2009) [arXiv:0810.1527]; H. Yuksel, M. D. Kistler and T. Stanev, Phys. Rev. Lett. **103**, 051101 (2009) [arXiv:0810.2784 [astro-ph]]; S. Profumo, Central Eur. J. Phys. **10**, 1 (2011) [arXiv:0812.4457 [astro-ph]]; D. Malyshev, I. Cholis and J. Gelfand, Phys. Rev. D **80**, 063005 (2009) [arXiv:0903.1310 [astro-ph.HE]].

[14] D. Grasso *et al.* [FERMI-LAT Collaboration], Astropart. Phys. **32** (2009) 140 [arXiv:0905.0636 [astro-ph.HE]]; T. Linden and S. Profumo, Astrophys. J. **772**, 18 (2013) [arXiv:1304.1791 [astro-ph.HE]]; P. -F. Yin, Z. -H. Yu, Q. Yuan and X. -J. Bi, Phys. Rev. D **88**, no. 2, 023001 (2013) [arXiv:1304.4128 [astro-ph.HE]].

[15] L. Bergstrom, T. Bringmann and J. Edsjo, Phys. Rev. D**78**, 103520 (2008); M. Cirelli and A. Strumia, PoS IDM **2008**, 089 (2008) [arXiv:0808.3867 [astro-ph]]; V. Barger *et al.*, Phys. Lett. B**672**,141 (2009); D. Hooper, A. Stebbins and K. M. Zurek, Phys. Rev. D **79**, 103513 (2009) [arXiv:0812.3202 [hep-ph]]. X. J. Bi, P. H. Gu, T. Li and X. Zhang, JHEP **0904**, 103 (2009); D. Hooper and K. M. Zurek, Phys. Rev. D **79**, 103529 (2009) [arXiv:0902.0593 [hep-ph]]; K. Cheung, P. -Y. Tseng and T. -C. Yuan, Phys. Lett. B **678**, 293 (2009) [arXiv:0902.4035 [hep-ph]]; C. -R. Chen, M. M. Nojiri, S. C. Park, J. Shu and M. Takeuchi, JHEP **0909**, 078 (2009) [arXiv:0903.1971 [hep-ph]]; D. S. M. Alves, S. R. Behbahani, P. Schuster and J. G. Wacker, Phys. Lett. B **692**, 323 (2010) [arXiv:0903.3945 [hep-ph]]; A. A. El-Zant, S. Khalil and H. Okada, Phys. Rev. D **81**, 123507 (2010) [arXiv:0903.5083 [hep-ph]]; M. Kuhlen and D. Malyshev, Phys. Rev. D **79**, 123517 (2009) [arXiv:0904.3378 [hep-ph]].

[16] S. Baek and P. Ko, JCAP **0910**, 011 (2009) [arXiv:0811.1646 [hep-ph]].

[17] P. Ko and Y. Omura, Phys. Lett. B **701**, 363 (2011) [arXiv:1012.4679 [hep-ph]].

[18] S. Baek, P. Ko, W. -I. Park and Y. Tang, arXiv:1402.2115 [hep-ph].

[19] C. R. Chen, F. Takahashi and T. T. Yanagida, Phys. Lett. B**671**, 71 (2009); Phys. Lett. B**673**, 255 (2009); C. R. Chen and F. Takahashi, JCAP **0902**, 004 (2009); P. F. Yin *et al.*, Phys. Rev. D**79**, 023512 (2009); K. Hamaguchi, E. Nakamura, S. Shirai and T. T. Yanagida, Phys. Lett. B **674**, 299 (2009) [arXiv:0811.0737 [hep-ph]]; A.Ibarra and D. Tran, JCAP **0902**, 021 (2009) [arXiv:0811.1555 [hep-ph]]; C. -R. Chen, M. M. Nojiri, F. Takahashi and T. T. Yanagida, Prog. Theor. Phys. **122**, 553 (2009) [arXiv:0811.3357 [astro-ph]]; E. Nardi, F. Sannino and A. Strumia, JCAP **0901**, 043 (2009) [arXiv:0811.4153 [hep-ph]]; A. Arvanitaki, S. Dimopoulos, S. Dubovsky, P. W. Graham, R. Harnik and S. Rajendran, Phys. Rev. D **79**, 105022 (2009)

[arXiv:0812.2075 [hep-ph]]; K. Hamaguchi, S. Shirai and T. Yanagida, Phys. Lett. B**673**, 247 (2009) [arXiv:0812.2374 [hep-ph]]; K. Ishiwata, S. Matsumoto and T. Moroi, Phys. Lett. B **675**, 446 (2009) [arXiv:0811.0250 [hep-ph]]; K. Ishiwata, S. Matsumoto and T. Moroi, JHEP **0905**, 110 (2009) [arXiv:0903.0242 [hep-ph]]; S. -L. Chen, R. N. Mohapatra, S. Nussinov and Y. Zhang, Phys. Lett. B **677**, 311 (2009) [arXiv:0903.2562 [hep-ph]]; A. Arvanitaki, S. Dimopoulos, S. Dubovsky, P. W. Graham, R. Harnik and S. Rajendran, Phys. Rev. D **80**, 055011 (2009) [arXiv:0904.2789 [hep-ph]].

[20] C. -H. Chen, C. -Q. Geng and D. V. Zhuridov, Phys. Lett. B **675**, 77 (2009) [arXiv:0901.2681 [hep-ph]]; JCAP **0910**, 001 (2009) [arXiv:0906.1646 [hep-ph]]; Eur. Phys. J. C **67**, 479 (2010) [arXiv:0905.0652 [hep-ph]].

[21] P. Minkowski, Phys. Lett. B **67**, 421 (1977); T. Yanagida, Proceedings of the Workshop on Unified Theories and Baryon Number in the Universe, edited by A. Sawada and A. Sugamoto, (KEK Report No. 79-18, 1979); S. Glashow, in Quarks and Leptons, Cargese, 1979, edited by M. Lévy *et al.* (Plenum, New York, 1980); M. Gell-Mann, P. Ramond, and R. Slansky, Proceedings of the Supergravity Stony Brook Workshop, New York, edited by P. Van Nieuwenhuizen and D. Freedman (North-Holland, Amsterdam, 1979); R. N. Mohapatra and G. Senjanović, Phys. Rev. Lett. **44**, 912 (1980).

[22] M. Magg and C. Wetterich, Phys. Lett. B **94**, 61 (1980); G. Lazarides, Q. Shafi and C. Wetterich, Nucl. Phys. B **181**, 287 (1981); R. N. Mohapatra and G. Senjanovic, Phys. Rev. D **23**, 165 (1981); E. Ma and U. Sarkar, Phys. Rev. Lett. **80**, 5716 (1998) [hep-ph/9802445].

[23] W. Konetschny and W. Kummer, Phys. Lett. B **70**, 433 (1977); J. Schechter and J. W. F. Valle, Phys. Rev. D **22**, 2227 (1980); T. P. Cheng and L. -F. Li, Phys. Rev. D **22**, 2860 (1980); S. M. Bilenky, J. Hosek and S. T. Petcov, Phys. Lett. B **94**, 495 (1980).

[24] E. Ma, Phys. Rev. D **73**, 077301 (2006) [hep-ph/0601225].

[25] R. Barbieri, L. J. Hall and V. S. Rychkov, Phys. Rev. D **74**, 015007 (2006) [hep-ph/0603188].

[26] L. Lopez Honorez, E. Nezri, J. F. Oliver and M. H. G. Tytgat, JCAP **0702**, 028 (2007) [hep-ph/0612275].

[27] A. Arhrib, Y. -L. S. Tsai, Q. Yuan and T. -C. Yuan, arXiv:1310.0358 [hep-ph].

[28] M. Gustafsson, E. Lundstrom, L. Bergstrom and J. Edsjo, Phys. Rev. Lett. **99**, 041301 (2007) [astro-ph/0703512 [ASTRO-PH]].

[29] E. Nezri, M. H. G. Tytgat and G. Vertongen, JCAP **0904**, 014 (2009) [arXiv:0901.2556 [hep-

ph]].

[30] Q. -H. Cao, E. Ma and G. Rajasekaran, Phys. Rev. D **76**, 095011 (2007) [arXiv:0708.2939 [hep-ph]].

[31] E. Dolle, X. Miao, S. Su and B. Thomas, Phys. Rev. D **81**, 035003 (2010) [arXiv:0909.3094 [hep-ph]]; X. Miao, S. Su and B. Thomas, Phys. Rev. D **82**, 035009 (2010) [arXiv:1005.0090 [hep-ph]].

[32] M. Aguilar *et al.* [AMS Collaboration], Phys. Rept. **366**, 331 (2002) [Erratum-ibid. **380**, 97 (2003)].

[33] O. Adriani *et al.* [PAMELA Collaboration], Phys. Rev. Lett. **105**, 121101 (2010) [arXiv:1007.0821 [astro-ph.HE]].

[34] Y. Asaoka, Y. Shikaze, K. Abe, K. Anraku, M. Fujikawa, H. Fuke, M. Imori and S. Haino *et al.*, Phys. Rev. Lett. **88**, 051101 (2002) [astro-ph/0109007].

[35] P. S. B. Dev, D. K. Ghosh, N. Okada and I. Saha, arXiv:1307.6204 [hep-ph].

[36] T. Han, B. Mukhopadhyaya, Z. Si and K. Wang, Phys. Rev. D **76**, 075013 (2007) [arXiv:0706.0441 [hep-ph]]. A. G. Akeroyd, M. Aoki and H. Sugiyama, Phys. Rev. D **77**, 075010 (2008) [arXiv:0712.4019 [hep-ph]]; A. G. Akeroyd and C. -W. Chiang, Phys. Rev. D **80**, 113010 (2009) [arXiv:0909.4419 [hep-ph]]; F. del Aguila and J. A. Aguilar-Saavedra, Nucl. Phys. B **813**, 22 (2009) [arXiv:0808.2468 [hep-ph]]; A. G. Akeroyd, C. -W. Chiang and N. Gaur, JHEP **1011**, 005 (2010) [arXiv:1009.2780 [hep-ph]]; A. G. Akeroyd and H. Sugiyama, Phys. Rev. D **84**, 035010 (2011) [arXiv:1105.2209 [hep-ph]]. A. Melfo, M. Nemevsek, F. Nesti, G. Senjanovic and Y. Zhang, Phys. Rev. D **85**, 055018 (2012) [arXiv:1108.4416 [hep-ph]]. M. Aoki, S. Kanemura and K. Yagyu, Phys. Rev. D **85**, 055007 (2012) [arXiv:1110.4625 [hep-ph]]. C. -W. Chiang, T. Nomura and K. Tsumura, Phys. Rev. D **85**, 095023 (2012) [arXiv:1202.2014 [hep-ph]]. H. Sugiyama, K. Tsumura and H. Yokoya, Phys. Lett. B **717**, 229 (2012) [arXiv:1207.0179 [hep-ph]]; S. Kanemura, K. Yagyu and H. Yokoya, Phys. Lett. B **726**, 316 (2013) [arXiv:1305.2383 [hep-ph]]. E. J. Chun and P. Sharma, Phys. Lett. B **728**, 256 (2014) [arXiv:1309.6888 [hep-ph]].

[37] P. Fileviez Perez, T. Han, G. -y. Huang, T. Li and K. Wang, Phys. Rev. D **78**, 015018 (2008) [arXiv:0805.3536 [hep-ph]].

[38] A. Arhrib, R. Benbrik, M. Chabab, G. Moultaka, M. C. Peyranere, L. Rahili and J. Ramadan, Phys. Rev. D **84**, 095005 (2011) [arXiv:1105.1925 [hep-ph]]; A. Arhrib, R. Benbrik, M. Chabab,

G. Moultaka and L. Rahili, JHEP **1204**, 136 (2012) [arXiv:1112.5453 [hep-ph]].

[39] F. del Aguila and M. Chala, JHEP **1403**, 027 (2014) [arXiv:1311.1510 [hep-ph]].

[40] S. Chatrchyan *et al.* [CMS Collaboration], Eur. Phys. J. C **72**, 2189 (2012) [arXiv:1207.2666 [hep-ex]].

[41] G. Aad *et al.* [ATLAS Collaboration], Eur. Phys. J. C **72**, 2244 (2012) [arXiv:1210.5070 [hep-ex]].

[42] B. Pontecorvo, Sov. Phys. JETP **6**, 429 (1957) [Zh. Eksp. Teor. Fiz. **33**, 549 (1957)].

[43] Z. Maki, M. Nakagawa and S. Sakata, Prog. Theor. Phys. **28**, 870 (1962).

[44] M. Kuhlen, M. Vogelsberger and R. Angulo, Phys. Dark Univ. **1**, 50 (2012) [arXiv:1209.5745 [astro-ph.CO]].

[45] R. Abbasi *et al.* [IceCube Collaboration], Phys. Rev. D **84** (2011) 022004 [arXiv:1101.3349 [astro-ph.HE]].

[46] M. G. Aartsen *et al.* [IceCube Collaboration], arXiv:1309.7007 [astro-ph.HE].

[47] J. Hisano, S. Matsumoto and M. M. Nojiri, Phys. Rev. Lett. **92**, 031303 (2004) [arXiv:hep-ph/0307216]; N. Arkani-Hamed, D. P. Finkbeiner, T. R. Slatyer and N. Weiner, Phys. Rev. D**79**, 015014 (2009) [arXiv:0810.0713 [hep-ph]].

[48] M. Pospelov and A. Ritz, Phys. Rev. D**78**, 055003 (2008) [arXiv:0803.2251 [hep-ph]]; D. Feldman, Z. Liu and P. Nath, Phys. Rev. D**79**, 063509 (2009) [arXiv:0810.5762v3 [hep-ph]]; J. D. March-Russell and S. M. West, Phys. Lett. B **676**, 133 (2009) [arXiv:0812.0559 [astro-ph]].

[49] A. Belyaev, N. D. Christensen and A. Pukhov, Comput. Phys. Commun. **184**, 1729 (2013) [arXiv:1207.6082 [hep-ph]].

[50] G. Belanger, F. Boudjema, A. Pukhov and A. Semenov, arXiv:1305.0237 [hep-ph]; G. Belanger, F. Boudjema, P. Brun, A. Pukhov, S. Rosier-Lees, P. Salati and A. Semenov, Comput. Phys. Commun. **182** (2011) 842 [arXiv:1004.1092 [hep-ph]]; G. Belanger, F. Boudjema, A. Pukhov and A. Semenov, arXiv:0803.2360 [hep-ph]; G. Belanger, F. Boudjema, A. Pukhov and A. Semenov, Comput. Phys. Commun. **176** (2007) 367 [arXiv:hep-ph/0607059].

[51] J. F. Navarro, C. S. Frenk and S. D. M. White, Astrophys. J. **462**, 563 (1996) [astro-ph/9508025].

[52] M. Cirelli, R. Franceschini and A. Strumia, Nucl. Phys. B **800**, 204 (2008) [arXiv:0802.3378 [hep-ph]].

[53] T. Bringmann and P. Salati, Phys. Rev. D **75**, 083006 (2007) [astro-ph/0612514].

[54] E. A. Baltz and J. Edsjo, Phys. Rev. D **59**, 023511 (1998) [astro-ph/9808243].

[55] E. A. Baltz, J. Edsjo, K. Freese and P. Gondolo, Phys. Rev. D **65**, 063511 (2002) [astro-ph/0109318].

[56] I. V. Moskalenko and A. W. Strong, Astrophys. J. **493**, 694 (1998) [astro-ph/9710124].